CNIC-01638/30
CNNC-0003

Calculation of the Nuclear Fission Data Based on the Framework of the QMD+SDM

RONG Jian
China Nuclear Data Center, China Institute of Atomic Energy
Beijing, 102413
O. Iwamoto T. Fukahori
Nuclear Data Center, Japan Atomic Energy Research Institute
Tokai-mura, Naka-gan, Ibaraki-Ken, 319-1195, Japan

Abstract: The quantum molecular dynamics (QMD), statistical decay model (SDM) and the statistical fission theory were used to analyze the mass distribution of the fission products, the prompt fission neutron spectrum ($\chi(E)$) and the prompt fission neutron multiplicities ($\overline{\nu}_{\mathrm{pf}}(E)$) caused by the intermediate energy nucleon-induced fission. The semi-empirical formula of energy level density parameter used in the statistical process was also studied. Very few adjustable parameters were included in the present method. By some physical analysis, it can be thought that the present results are reasonable. The $\chi(E)$ and $\overline{\nu}_{\mathrm{pf}}(E)$ can be obtained in the intermediate energy region by the present method.

Key words: QMD, SDM, Prompt fission neutron spectrum, Prompt fissio neutron Multiplicities

INTRODUCTION

For the design of the accelerator-driven subcritical system (ADS) and some other applications, it is important to know the prompt fission neutron spectrum $\chi(E)$ and the average prompt neutron multiplicities $\overline{\nu}_{\mathrm{pf}}(E)$ as the function of the incident energy, resulting from the intermediate energy neutron induced fission. The fission reactions by the intermediate energy incident neutron can be considered as a two-step process. In the first step, the nucleon-nucleon collisions inside the nucleus induce the emission of several nucleons and lead the formation of an excited pre-fission nucleus. In the second step, the pre-fission nucleus deexcites by fission. Recently, a unified method based on quantum molecular dynamics[1] (QMD) plus statistical decay model (SDM) including the relativistic correction and high energy fission had been developed to research the nuclear reaction in the intermediate energy region[2,3]. In this energy region, the whole reaction process can be divided into two parts that can be separated in their typical reaction time scales. For the first part, which was named the dynamical process, the order of the typical collision times is less than 10^{-21} second, and the main reactions during this process are the direct reaction and the pre-equilibrium reaction. After that it is a statistical process that order of the time scale is the 10^{-21}～10^{-15} second and the main reactions are the evaporation and fission. In order to analyze, the two- step model of QMD+SDM can be used: QMD is used for the dynamical process and SDM is used for the statistical one. For the fission by the intermediate energy neutron the distribution of the pre-fission nucleus and their excited energy can be calculated by the above method.

There were lots of work about the prompt fission neutron spectrum $\chi(E)$ and the average prompt neutron multiplicities $\bar{\nu}_{\rm pf}(E)$ in the past year[4~6] in the energy region below 20 MeV. Most of calculations of $\chi(E)$ in this work are based on either Maxwellian or Watt spectrum with some adjustable parameters to fit the experimental data for the given fission nucleus at a given excitation energy. In the above two kinds of distribution functions, neglected are the distribution of fission-fragment temperature that resulted from the initial distribution of fission-fragment excitation energy and the subsequent cooling of the fragments by neutron emission. For the fission reaction resulting from the low energy neutrons these methods are acceptable because of the small number of the emitted neutrons from the fission (see the reference [6] and the papers cited in it). But for the fission resulting from the incident neutron with the energy higher than several tens MeV, this assumption no longer works. When the incident energy of the neutron is high enough (above the multiple-chance fission threshold), several nucleons would be emitted before the fission occurred. The pre-fission nuclei and their excitation energy distributions have some kinds of distributions for the difference of target and incident energy of the neutron. The examples of distributions of mass-charge and excitation energy of pre-fission nuclei are shown in Fig. 1 (calculated by QMD). Because of the high excitation energy, more neutrons can be emitted from the fissile nuclei to deexcite. The prompt neutron energy spectrum depends strongly on the distribution of fission fragment excitation energy.

The Hauser-Feshbach theory was used to calculate the prompt spontaneous fission neutron spectrum of the ^{252}Cf [7]. This method improved some deficiencies of the Watt and Maxwellian spectra, but it has some difficulty to use for nucleon induced fission reaction in the intermediate energy region.

Based on the nuclear evaporation theory [8], D. G. Madland and J. R. Nix derived a model [9] to calculate the fission neutron energy spectrum, taking into account the cooling of the fragments by neutrons emission. Unphysical adjustment parameters, which are used in the Maxwellian or Watt spectrum to fit the experiment data, are not necessary in this model.

In the present work, we used the two-step process to analyze the prompt fission neutron spectrum $\chi(E)$ and the average prompt neutron multiplicities $\bar{\nu}_{\mathrm{pf}}(E)$ resulting from the intermediate energy neutron induced fission. QMD was used at first to analyze the dynamical process. And then the statistical process was taken into account. The SDM can be used to calculate distribution of the pre-fission nuclei and its excitation energy after the calculation of QMD. Using the statistical fission theory [10] the distributions of the fission-fragments and their excitation energies can be obtained. And then these distributions can be used in the Madland-Nix model to get the $\chi(E)$ and $\bar{\nu}_{\mathrm{pf}}(E)$. In Sec. 1 we describe simply the QMD, SDM, statistical fission method, and Madland-Nix model what will be used in the present work. In Sec. 2 we give some calculated results. Because of lacking the experimental results, we just can do some physical analysis for our calculations. The summary and conclusion of this work will be given in Sec. 3.

1 DESCRIPTION OF THE CALCULATION MODEL

1. 1 Quantum molecular dynamics

The details of the QMD theories are given in Ref. [1]. QMD is an approach that incorporates some relativistic and quantum features, like the Pauli principle, many-body system by using mean field theory, relativistic correction, etc., into the N-body phase space dynamics of the classical molecular dynamics method[11]. In this model, each nucleon state is represented by a Gaussian wave packet function with a width L of the spatial spread.

$$f_i(\boldsymbol{r},\boldsymbol{p},t)=\frac{1}{(\pi\hbar)^3}\exp(-\frac{(\boldsymbol{r}-\boldsymbol{r}_{i0}(t))^2}{2L}-(\boldsymbol{p}-\boldsymbol{p}_{i0}(t))^2\frac{2L}{\hbar^2}) \tag{1}$$

where $\boldsymbol{r}_{i0}$ and $\boldsymbol{p}_{i0}$ are the centroid of particle i in coordinate and momentum space, respectively. The n-body Hamiltonian can be defined as,

$$\mathrm{H}=\sum_i T_i+V_i \tag{2}$$

where T_i is the kinetic energy and V_i is the potential energy of the mean field, which is given by local Skyrem two and three particle interactions, Yukawa, Coulomb, the momentum dependent interaction, and the Pauli potential [12].

$$V=V^{\mathrm{loc}}+V^{\mathrm{Yuk}}+V^{\mathrm{coul}}+V^{\mathrm{MDI}}+V^{\mathrm{Pauli}} \tag{3}$$

$$V^{\mathrm{loc}}=t_1\,\delta(\boldsymbol{r}_1-\boldsymbol{r}_2)+t_2\,\delta(\boldsymbol{r}_2-\boldsymbol{r}_2)\delta(\boldsymbol{r}_1-\boldsymbol{r}_3)$$

$$V^{\mathrm{coul}}=c_1c_2\frac{e^2}{\mathrm{abs}(\boldsymbol{r}_1-\boldsymbol{r}_2)}\mathrm{erf}(\mathrm{abs}(\boldsymbol{r}_1-\boldsymbol{r}_2)/\sqrt{4L})$$

$$V^{\mathrm{Yuk}}=t_3\exp(\mathrm{abs}(\boldsymbol{r}_1-\boldsymbol{r}_2)/a)/\mathrm{abs}(\boldsymbol{r}_1-\boldsymbol{r}_2)$$

$$V^{\mathrm{MDI}}=t_4\ln^2(t_5(\boldsymbol{p}_1-\boldsymbol{p}_2)^2+1)\delta(\boldsymbol{r}_1-\boldsymbol{r}_2)$$

$$V^{\mathrm{Pauli}}=v_{\mathrm{p}}(\frac{\hbar}{p_0q_0})^2\exp(-(\boldsymbol{r}_1-\boldsymbol{r}_2)^2/2q_0{}^2-(\boldsymbol{p}_1-\boldsymbol{p}_2)^2/2p_0{}^2)$$

where erf denotes the error function. The parameters in the above equations can be determined by the ground properties of infinite nuclear matter and c_i

is 0 for neutrons and 1 for protons.

We should select a suitable switching time to determine when the QMD calculation should be terminated and the statistic calculation could be started. The switching time should be long enough so that the fragment productions can be achieved to stable values by the QMD calculation. By the investigation of the reaction time scale of the preequilibrium reaction for intermediate-energy nuclear reactions in terms of QMD, it had been found[13] that the 100 fm/c was the suitable switching time. It means that after 100 fm/c the system is already in the well thermally equilibrated stage and can be treated by the statistical methods.

1. 2 Statistical process

Many fragments normally in highly excited states are created after the QMD simulation. The decay of the fragment is taken place by emitting several nucleons and light ions or fission process. The fragments are all in the thermal equilibrated states so it can be treated by the statistical decay method. With the evaporation model the emission probability P_x of the light-particle x is as fellow:

$$P_x = (2J_x + 1) m_x \varepsilon \sigma_x(\varepsilon) \rho(E^*) \mathrm{d}\varepsilon \tag{4}$$

where J_x, m_x, and ε are the spin, mass and kinetic energy of the particle x (in this work the x = n, p, d, t, ^{3}He and α particle). The $\sigma_x(\varepsilon)$ and the $\rho(E^*)$ denote the inverse cross section for the absorption of the particle with energy ε and the level density of the residual nucleus with the excitation energy E^*, respectively. If the excitation energy is larger than the fission threshold the fission reaction is occurred. A very simple form of $\rho(E^*)$ is used in this work:

$$\rho(E^*) = \text{const.} * \exp(2(aE^*)^{1/2}) \tag{5}$$

where a is the level density parameter. As usual, it can be used in the following relationship:

$$a = A/8 \quad (\text{MeV}^{-1}) \tag{6}$$

where A is the mass number of the nuclei. In the calculation of the $\chi(E)$ and $\bar{\nu}_{\text{pf}}(E)$, Madland and Nix changed the above relationship into the $a = A/11$ [9], which is better for the fission productions. In the present work, a new empirical formula is used. This formula is related with the nucleon incident energy and it is derived in Sec. 2.

After some light-particle emission we can get the pre-fission nuclei. The Takahashi's statistical fission model [14] is used to get the fission product nuclei distribution. By this model and the neglecting the deformation energy, the distribution function for the produced fission fragments (A_1, Z_1) and (A_2, Z_2) from the pre-fission nuclei (A, Z) can be written as

$$D(A,Z,A_1,Z_1,A_2,Z_2) \propto \frac{(a_1a_2)^{1/2}}{(a_1+a_2)^{13/4}}\left(\frac{A_1^{5/3}A_2^{5/3}}{A_1^{5/3}+A_2^{5/3}} * \frac{A_1A_2}{A_1+A_2}\right)^{3/2} *$$

$$\left(\frac{Z_{p1}Z_{p2}}{B_{A1}+B_{A2}-\frac{K}{Z_1Z_2}}\right)^{1/2} E^{*\,11/4}\left(1-\frac{5}{2}\frac{1}{((a_1+a_2)E^*)}\right) * \tag{7}$$

$$\exp(2((a_1+a_2)E^*)^{1/2})$$

where E^* is the excitation energy and K is the total fission fragment kinetic energy. In Eq. (7)

$$B_{Ai} = 0.041505/Z_{Ai} \tag{8}$$

$$Z_{\mathrm{p1}} = \frac{B_{A1}Z_{A1} - B_{A2}Z_{A2} + Z\left(B_{A2} - \frac{K}{2Z_1Z_2}\right)}{B_{A1} + B_{A2} - \frac{K}{Z_1Z_2}} \tag{9}$$

$$Z_{\mathrm{p2}} = Z - Z_{\mathrm{p1}} \tag{10}$$

$$Z_{Ai} = A_i \big/ (1.98067 + 0.0149624A_i^{2/3}) \tag{11}$$

And

$$a_i = a * A_i \tag{12}$$

where i is 1 and 2 in these formula and a is the level density parameter which is showed in Eq. (24).

The total fission fragment kinetic energy K can be obtained from the systematics method [15] as

$$K = 0.1189 Z^2 / A^{1/3} + 7.3 \text{ (MeV)} \tag{13}$$

For the spontaneous fission the excitation energy E^* of fragment is expressed by

$$E^* = E_{\mathrm{r}}^* - K \tag{14}$$

where the E_{r}^* is the average energy release from the fission.

1. 3 Prompt neutron energy spectra and prompt neutron multiplicities

The details of the Madland-Nix model for the prompt neutron energy spectrum are described in Ref. [9]. By the Fermi gas model the relationship between the excitation energy E^* and the nuclear temperature T is as

$$E^* = aT^2 \tag{15}$$

where the a is the level density parameter. The distribution of nuclear temperature T in the nuclear system is approximated by the triangular distribution. The maximum temperature T_{m} is related to the E^* approximately by

$$T_{\mathrm{m}} = (E^*/a)^{1/2} \tag{16}$$

and the E^* can be given by the Eq. (14). In the center-of-mass system the neutron energy spectrum is expressed as

$$\chi(\varepsilon) = \frac{2\varepsilon}{T_{\mathrm{m}}^2} E_1(\varepsilon/T_{\mathrm{m}}) \tag{17}$$

where

$$E_1(x) = \int_x^\infty \frac{\exp(-u)}{u} \mathrm{d}u$$

is the exponential integral [16].

The excited fission fragments decay by emission of the fission neutrons and prompt gamma. By the energy conservation the total average fission-fragment excitation energy $\langle E^* \rangle$ is equal to the product of the average prompt neutron multiplicity $\bar{\nu}_{\mathrm{pf}}$ and the average energy emission per emitted neutron

$\langle\eta\rangle$ plus the average prompt gamma energy $\langle E_\gamma\rangle$. The $\langle\eta\rangle$ is represented [17] reasonably well by the sum of the average fission-fragment neutron separation energy $\langle S_{pn}\rangle$ and the average center-of-mass energy of the emitted neutrons $\langle\varepsilon\rangle$. By the Eq. (17) we can get

$$\langle\varepsilon\rangle = \int_0^\infty \varepsilon\chi(\varepsilon)\mathrm{d}\varepsilon = \frac{4}{3}T_{\mathrm{m}} \tag{18}$$

This yields the form

$$\nu_{\mathrm{pf}} = \frac{\langle E_{\mathrm{r}}^*\rangle - \langle K\rangle - \langle E_\gamma\rangle}{\langle S_{\mathrm{pn}}\rangle + \frac{4}{3}T_{\mathrm{m}}} \tag{19}$$

The $\langle S_{pn}\rangle$ can be calculated as with the same method for calculation of the average energy release discussed in Eq. (14). Hoffman et al. gave a review [18] about the $\langle E_\gamma\rangle$. For some typical value, the 8 MeV of the average prompt gamma energy $\langle E_\gamma\rangle$ per fission is available [19].

2 CALCULATIONS AND RESULTS

In this section, the fission product mass distribution by the two reactions, p (1GeV)+^{197}Au and p (800 MeV)+^{208}Pb, and the prompt neutron spectrum and average prompt neutron multiplicities resulting from the following reactions, n (150 MeV, 500 MeV, 1GeV, 1.5GeV, 2GeV, 3GeV)+^{238}U(^{239}Pu, ^{246}Cm), are calculated by the above method.

The level density parameter *a* is a very important parameter for the statistical process. In the Fig. 2 it can be found that the systematics relationship *a*=*A*/(8 MeV) is very good to represent the level density parameter for almost all the heavy nuclei and fissionable nuclei. From this figure it also can be found that *a* is varied with the mass number *A*. For the fission products, the mass of them is near 90 (for light part) and 140 (for heavy part). Therefore the systematics should be changed to use *a*=*A*/10 due to the shell structure effect. These conclusions are completely based on the assumption that the nuclei are in the ground state. As usual, residual nuclei with excitation energy up to several hundreds MeV can be produced in the reactions of intermediate energy nucleon. With the excitation energy increasing, the level density should be deduced [24]. By the phenomenological analysis [25] this conclusion is also right and the values of the level parameter $a=A/10\sim A/15$ are reasonable.

At the same time, the semi-empirical level density parameter a is written as following [26]

$$a=\gamma_1 A+\gamma_2 B_s A^{2/3} \quad (\text{MeV}) \tag{20}$$

where B_s is the parameter about the surface area of the deformed nucleus and the γ_1 and γ_2 are two coefficients. As an approximation, B_s is related with the excitation energy of the nuclei in the surface area. It can be written as,

$$B_s \propto \frac{E^*}{A} * A^{2/3} \propto E^* * A^{-1/3} \tag{21}$$

Where the E^* is the total excitation energy of the pre-fission nuclei, which is approximately increased with the induced nucleon energy E. So the B_s can be written approximately as following

$$B_s \propto E * A^{-1/3} \tag{22}$$

From the Eq. (20) and (22), the level density parameter can be written as following,

$$a=\gamma_1 A+\gamma_2{}^* * E * A^{1/3} \quad (\text{MeV}) \tag{23}$$

Transferred it into the form of $a=A/8$ and the systematics of level density parameter, as shown in Fig. (2), we can get

$$a = A \big/ (\gamma_1' + \gamma_2' * E * A^{-2/3}) \equiv A/x' \quad (\text{MeV}) \tag{24}$$

where A is the mass of nuclei, E is the energy of the incident nucleon, and the γ_1' and γ_2' are two phenomenological parameters. In this work the values of γ_1' and γ_2' are selected as 10 and 0.036, respectively, that make the $a=A/10\sim A/13$.

Fig. 3(a) and 3(b) show the mass spectrum of fission fragments of 1 GeV proton bombarding ^{197}Au and 800 MeV proton bombarding ^{208}Pu, respectively. The two experiments include the mass distribution of the total fragments including the results of the fission and spallation reaction. But the two regions of products nuclei can be distinguished because the fission fragments' mass are approximately a half of the mass of the target and the spallation products are in the vicinity of the target. In the Fig. 3(b) we can find a two-peak structure, in Fig. 3(a) this kind of structure becomes ambiguous because of the higher incident energy.

Fig. 4, 5 and 6 show the fission prompt neutron energy spectra $\chi(E)$ of the ^{238}U, ^{239}Pu and ^{246}Cm bombarded by the intermediate energy neutron, respectively. The ^{238}U and ^{239}Pu ($T_{1/2} = 2.41\times10^4$ year(α)) are the important fissioning materials in ADS and the ^{246}Cm ($T_{1/2} = 4700$ year(α)) is the important actinide nuclide that needed to be transmuted. The prompt fission neutron multiplicities $\bar{\nu}_{\rm pf}(E)$ of the above mentioned nuclei are presented in the Table 1 and illustrated in Fig. 7. From the table it can be found that the $\bar{\nu}_{\rm pf}(E)$ for each nuclide would be approached to a saturated value and also we can find from Table 1 and Figs. 4～6 of $\chi(E)$ that the higher energy of the bombarding particle causes the higher average energy of the fission products. From the Fig. 7 it can be found that relationship between the $\bar{\nu}_{\rm pf}(E)$ and the E is not linear. The increase of the $\bar{\nu}_{\rm pf}(E)$ becomes slowly with the increase of the energy of incident neutron. The emitted neutrons with high energy can bring out more excitation energy from the excited fission products. That is why there is an upper limit of the $\bar{\nu}_{\rm pf}(E)$.

3 SUMMARY AND DISCUSSION

Based on the two steps reaction theory, we have calculated the prompt fission neutron energy spectrum and the fission neutron multiplicities in the intermediate energy region. The mass distribution of fission products can also be calculated in this frame. The calculated results are compared with the experiments (see Fig. 3).

We also have studied the semi-empirical formula of level density parameter as a function of incident energy for the statistical process of the intermediate energy nuclear reactions. It just needs two adjustable parameters, the γ_1' and γ_2' in Eq. (24), to fit the data of the fission neutron spectrum in the present work. Now it is not found any experimental results about the $\bar{\nu}_{\rm pf}(E)$

and $\chi(E)$ for the fission in the intermediate energy region. The Fig. 8 shows the calculated results by the present method (red, solid line) and the more rigorous method, the Monte-Carlo method (black, dashed line). It cannot be found any obviously different between the two methods. From this comparison shown in Fig. 8, it can be found that the Eq. 24 is a suitable empirical formula for the level density parameter and the parameters selected in the present work are suitable.

The results of the $\bar{\nu}_{\text{pf}}(E)$ and $\chi(E)$ are shown in Fig. 4 ～ 8 and Table 1. The QMD plus SDM was used to analysis the mass and excitation energy distribution of the pre-fission nuclei. And taking into account the cooling of the fission fragments by neutrons emission, the Madland-Nix model was used to calculate the $\bar{\nu}_{\text{pf}}(E)$ and $\chi(E)$. By adjusting the parameter γ_1' and γ_2' defined in Eq. 24, we can get the reasonable results about the fission reactions in the intermediate energy region.

Table 1 The table for the prompt fission neutron multiplicities and nuclear temperature T_m for the fission by the intermediate energy neutron

E_{in}/GeV	^{238}U		^{239}Pu		^{246}Cm	
	T_m/MeV	$\bar{\nu}_{pf}$	T_m/MeV	$\bar{\nu}_{pf}$	T_m/MeV	$\bar{\nu}_{pf}$
0.150	2.0821	13.7631	2.1086	13.3146	2.1085	13.9032
0.50	2.5022	19.6695	2.5434	19.4171	2.5707	20.3273
1	3.1111	27.4409	3.0888	26.3369	3.1217	28.0438
1.5	3.3761	31.4916	3.4262	30.9312	3.4958	32.8062
2	3.6962	35.8636	3.6187	33.6695	3.7582	36.3161
3	3.9436	38.1268	3.9478	36.6440	4.1202	40.1690

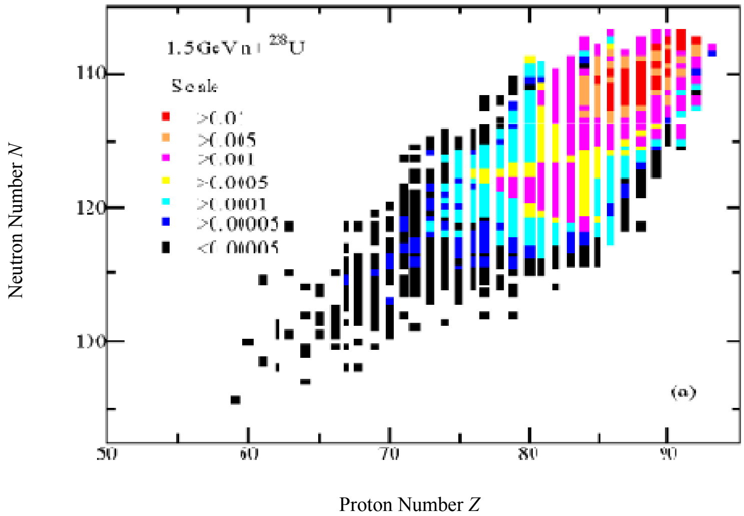

Fig. 1(a) and (b) are the distributions of the pre-fission nuclei in the *Z*-*N* plane and (c) and (d) are the distributions of the excitation energy in the energy-A plane for the 1.5 GeV n+^{238}U and 3 GeV n+^{238}U, respectively

The scale in these figures mean the yields. The same scale is also used in the figure 1(b), 1(c) and 1(d)

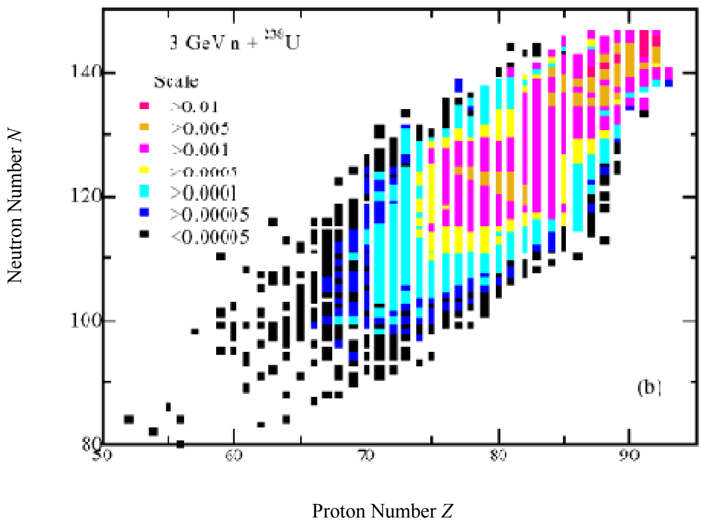

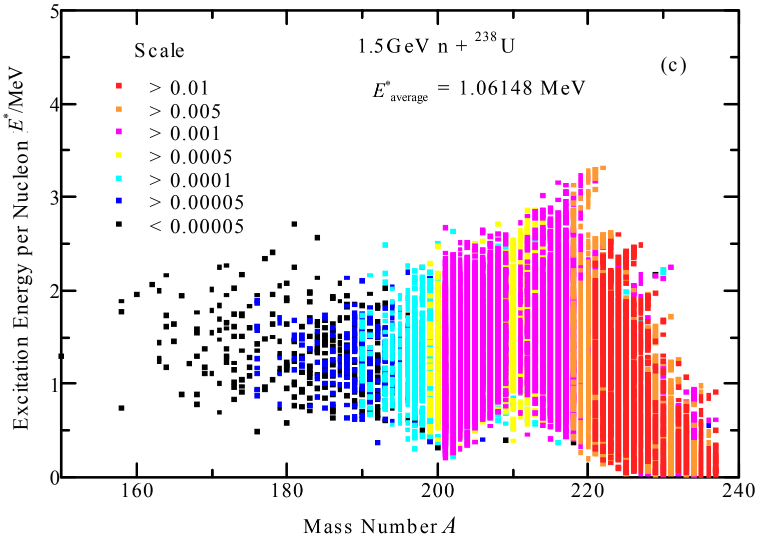
Scale
> 0.01
> 0.005
> 0.001
> 0.0005
> 0.0001
> 0.00005
< 0.00005
1.5GeV n + ^{238}U
$E^*_{average}$ = 1.06148 MeV
(c)
Excitation Energy per Nucleon E^*/MeV
Mass Number A

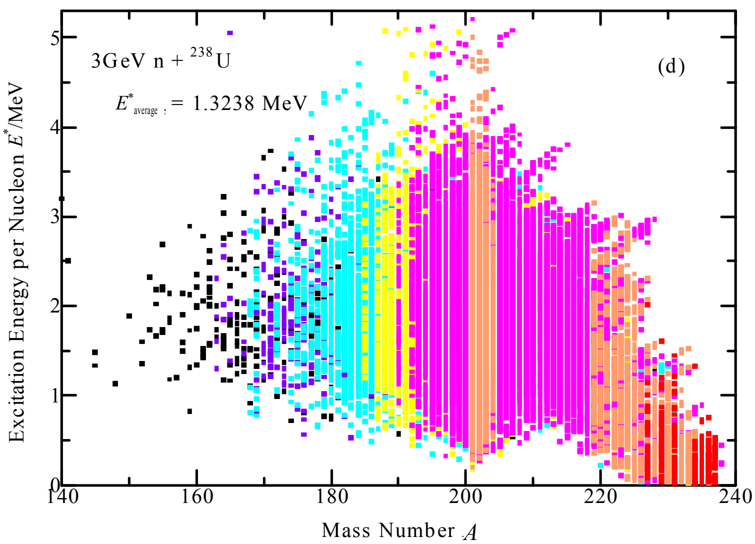
3GeV n + ^{238}U
$E^*_{average}$ = 1.3238 MeV
(d)
Excitation Energy per Nucleon E^*/MeV
Mass Number A

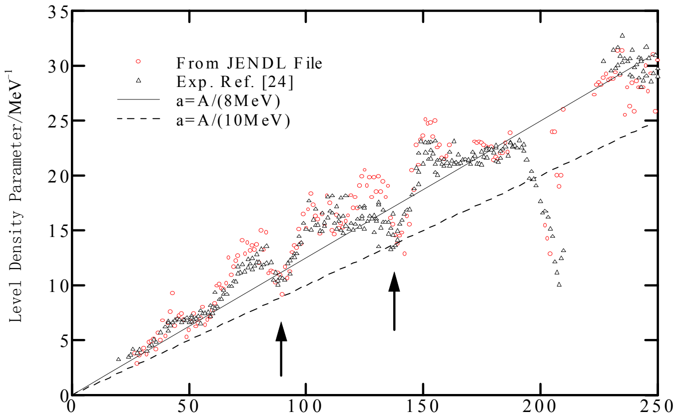

Fig. 2 Fermi gas level density parameter (a) for the data from JENDL[20] (open circle, provided by the Gibert-Cameron formula[21]) and the experiment[24] (open triangle) and two systemastic linear relationship. As usual these points are best represented on the average by the solid line corresponding to a=A/(8 MeV). But for the fission-fragments nuclei we should use the relationship a=A/(10 MeV) because their mass is positioned at arround the 90 and 140 (arrow)

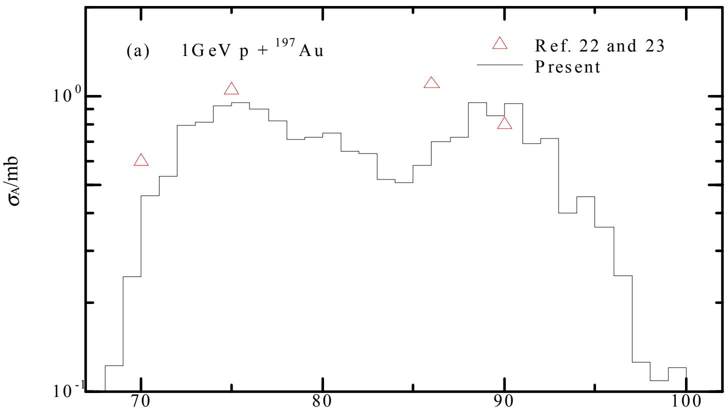

Fig. 3 Fission product nuclei mass spectrum. Theoretical results are obtained by the QMD plus statstical fission model

(a) is the result of p(1 GeV)+^{197}Au and (b) is the result of the p(800 MeV)+^{208}Pb

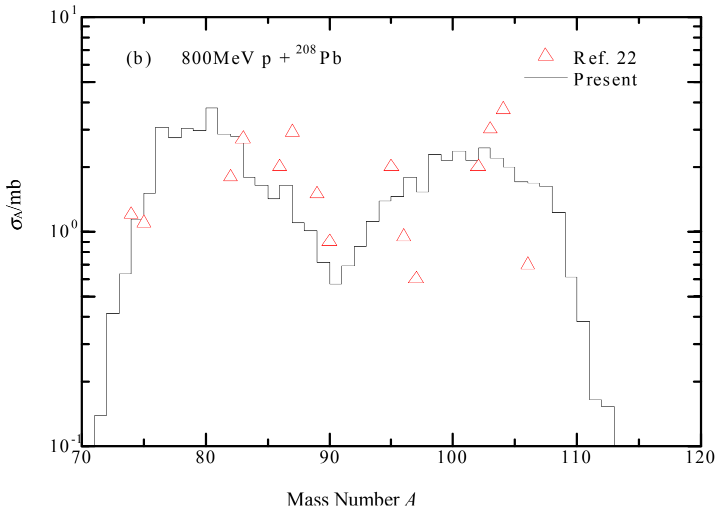

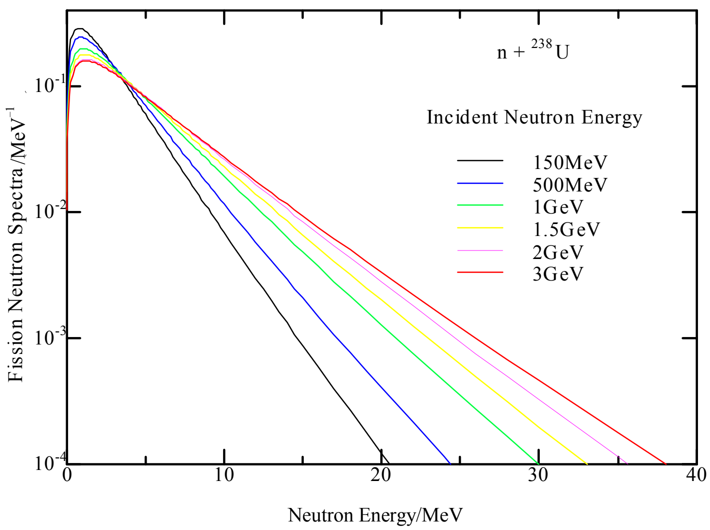

Fig. 4 Fission neutron spectra in the center-of-mass system for the fission of ^{238}U by intermediate energy neutron. The nuclei temperature and average prompt neutron multiplicities for each incident energy are listed in Table 1

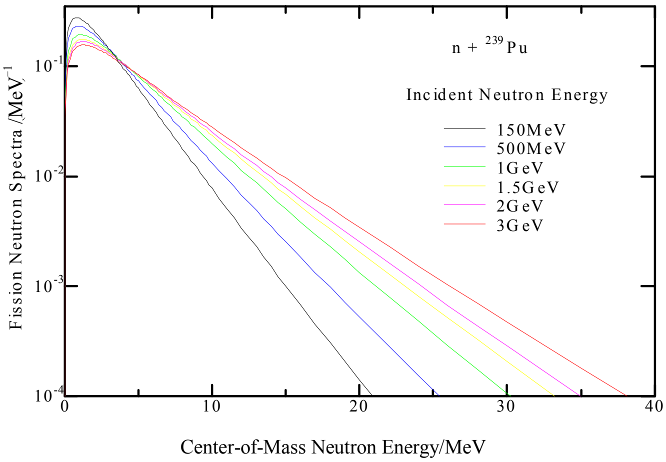

Fig. 5 Fission neutron spectra in the center-of-mass system for the fission of ^{239}Pu by intermediate energy neutron. The nuclear temperature and prompt fission neutron multiplicities for each incident energy are listed in Table 1

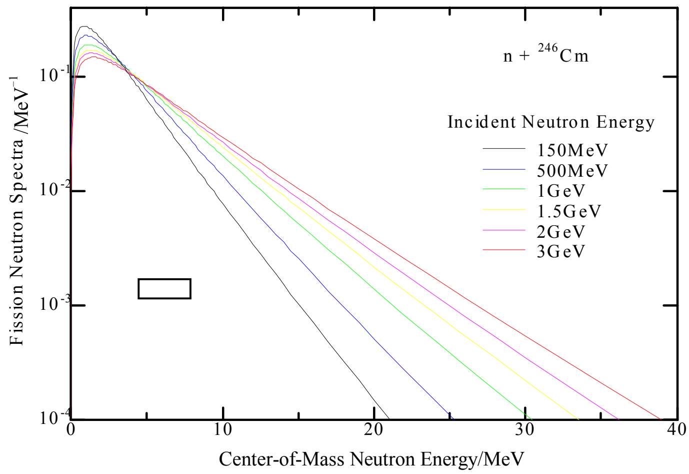

Fig. 6 Fission neutron spectra in the center-of-mass system for the fission of ^{246}Cm by intermediate energy neutron. The nuclear temperature and prompt fission neutron multiplicities for each incident energy are listed in Table 1

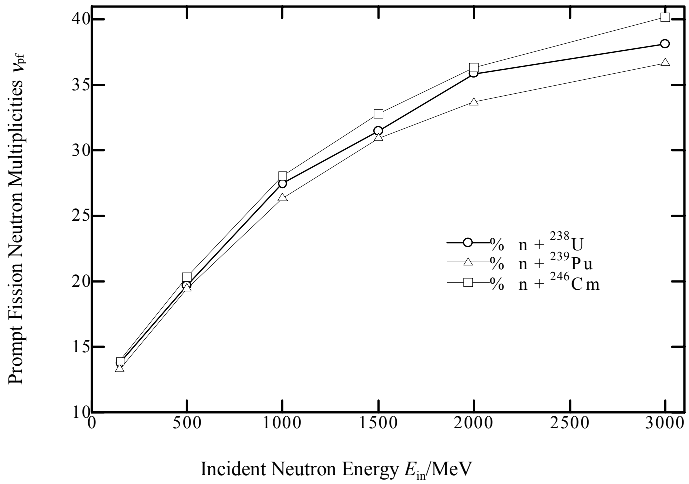

Fig. 7 Relation between ν_{pf} and the incident neutron energy (E_{in}) for ^{238}U, ^{239}Pu and ^{246}Cm. It is clear that the higher E_{in} can create the more fission neutron. It can be also found that ν_{pf} has the trend of the saturation according to increasing the incident energy

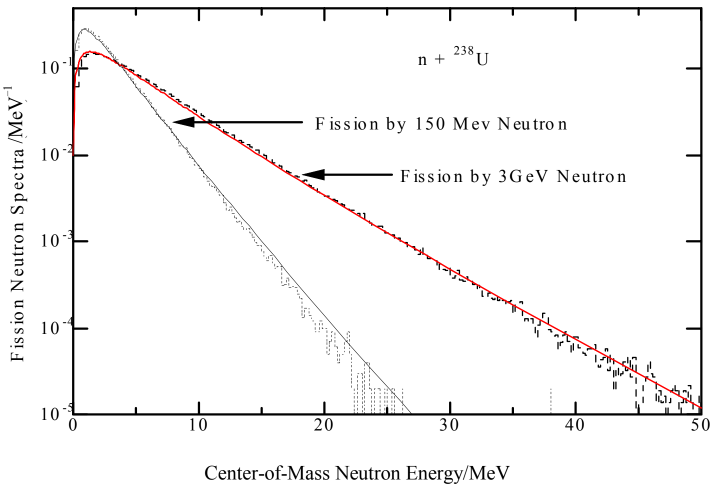

Fig. 8 Prompt neutron spectra in the center-of-mass system for the fission by 150 MeV and 3 GeV neutrons, respectively

The spectrum shown by red, solid line is calculated from Eq. (17) and the black, dashed one is calculated by the Monte-Carlo method (by QMD). There isn't any large difference between the two results

REFERENCE

1 Aichelin J. Phys. Rep. 1991, 202: 233

2 Niita K. Chiba S. Maruyama T. et al. Phys. Rev. 1995, C52: 2620

3 Chiba S, Iwamoto O, Fukahori T, Niita K, Maruyama T, Maruyama T, Iwamoto A. Phys. Rev. 1996, C54: 285

4 Terrell J. Phys. Rev., 1959, 113: 527

5 Howerton R. J. Nucl. Sci. Eng., 1977, 62: 438

6 Baba M. Wakabayashi H. Ito N. Maeda K. and Hirakawa N. J. Nucl. Sci. Tech., 1990, 27[7]: 601

7 Browne J C. and Dietrich F S. Phys. Rev. 1974, C10: 2545

8 Weisskoff V F. Phys. Rev., 1937, 52: 295

9 Madland D G. and Nix J R. Nucl. Sci. Eng., 1982, 81: 213

10 Fong P. Phys. Rev., 1953, 89: 332, Phys. Rev., 1956, 102: 434

11 Sangster T C. Britt H C. Fields D J. Hansen L F. Lanier R G. Namboodiri M N. Remington B A. Webb M L. Begemann-Blaich M. Blaich T. Fowler M M. Wilhelmy J B. Chan Y D. Dacal A. Harmon A. Pouliot J. Stokstad R G. Kaufman S. Videbaek F. Fraenkel Z. Peilert G. Stoeker H. Greiner W. Botvina A. and Mishustin I N. Phys. Rev. 1992, C46: 1404

12 Hartnack C. Li Z. Neise L. Peilert G. Rosenhauer A. Sorge H. Aichelin J. Stoecker H. and Greiner W. Nucl. Phys. 1989, A495: 303c

13 Chiba S. Niita K. and Iwamoto O. Phys. Rev. 1996, C54: 3302

14 Takahashi H. Nucl. Sci. Eng., 1984, 87: 432

15 Viola V E. Kwiatkowski K. and Walker M. Phys. Rev., 1985, C31: 1550

16 Abramowitz M. and Stegun I A. Handbook of Mathematical Functions with Formulas, Graphs and Mathematical Tables, Chapter 5, Dover Publication, INC. New York, 1970

17 Terrell J. Phys. Rev., 1957, 108: 783

18 Hoffman D C. and Hoffman M M. Ann. Rev. Nucl. Sci., 1974, 24: 151

19 Vandenbosch R. and Huizenga J R., *Nuclear Fission, Chapter XIII*, Academic Press, New York and London, 1973

20 Shibata K. Nakagawa T. Asami T. Fukahori T. Narita T. Chiba S. Mizumoto M. Hasegawa A. Kikuchi Y. Nakajima Y. and Igarasi S. “Japanese Evaluated Nuclear Data Library, version-3”, JAERI-1319 (1990)

21 Gilbert A. and Cameron A G W. Can. J. Phys., 1965, 43: 1446

22 Cugnon J. Volant C. and Vuillier S. Nucl. Phys. 1997, A620: 475

23 Kaufman S B. and Steinberg E P. Phys. Rev. 1980, C22: 167

24 Junghans A R. De Jong M. Clerc H.-G. Ignatyuk A V. Kudyaev G A. and Schmidt K.-H. Nucl. Phys. 1998, A629: 635

25 Iljinov A S. Mebel M V. Bianchi N. De Sanctis E. Guaraldo C. Lucherni V. Muccifora V. Polli E. Reolon A. R. and Rossi P. Nucl. Phys. 1992, A543: 517

26 Ignatyuk A V. Itkis M G. Okolovich V N. Smirekin G N. and Tishin A S. Yad. Fiz. 1975, 21: 1185 (Sov. J. Nucl. Phys. 1975, 21: 612

QMD+SDM 方法计算中能核裂变数据

荣 健

中国核数据中心，北京 102413，中国

岩本 修 深崛 智生

日本核数据中心，那珂郡东海村，茨城县 319-1195，日本

摘 要：采用量子分子动力学(QMD)和统计衰变模型(SDM)分析计算了中能中子入射锕系核素引起裂变的瞬发裂变中子数和裂变中子谱。同时给出了用于本计算的一个简单的半经验的能级密度参数公式。这样，仅需要很少的输入参数便可得到合理的结果。

关键词：量子分子动力学 统计衰变模型 瞬发裂变中子数
裂变中子谱